

# Spin-1 bosons in an external magnetic field and a three body interaction potential

Sk Noor Nabi and Saurabh Basu\*

*Department of Physics, Indian Institute of Technology Guwahati, Guwahati, Assam 781039, India*

(Dated: November 18, 2018)

We perform a thorough study of the effect of an external magnetic field on a spin-1 ultracold Bose gas via mean field approach corresponding to the both signs of the spin dependent interaction. In contrast to some of the earlier studies, the magnetic field in our work is included through both the hopping frequencies (via Peierls coupling) and the zeeman interaction, thereby facilitating an exploration for competition between the two. The phase diagrams in the antiferromagnetic case shows that the Mott insulating (MI) phase with even particle occupancies is stable at low magnetic fields. At higher magnetic fields, due to a competition between the hopping and the zeeman interaction terms, the latter tries to destabilize the MI phase by suppressing the formation of singlet pairs, while the former tends to stabilize the MI phase. In the ferromagnetic case, the MI lobes become more stable with increasing flux strengths. Further inclusion of a three body interaction potential in order to ascertain its role on the phase diagram, we found that in absence of the magnetic field, the MI lobes become more stable compared to the superfluid (SF) phase and the location of the transition point for the MI-SF phase increases with increasing the three body interaction strength. A strong coupling perturbative calculation has also been done to provide a comparison with our mean field phase diagrams. Lastly, with inclusion of the external field, the insulating phases are found to be further stabilized by the three body interaction potential.

## I. INTRODUCTION

The experimental realization of the transition from a SF to MI in a system of neutral alkali atoms trapped in optical lattices has marked an important milestone towards exploring the many body phenomena in systems which demonstrate quantum phase transition [1]. Usage of two or more counter propagating laser beams, which form the optical lattice potential, allows one to have a precise control of the lattice parameters and the interaction potential between the constituent particles experimentally. These technological advancements have made the scientists capable to navigate through a myriad of interesting physical phenomena that are otherwise inaccessible in crystalline solids. The cooling of atoms involves sophisticated trapping techniques that are either magnetic or optical in nature.

In magnetic trapping, ultracold atoms are forced to have their internal atomic states frozen and hence behaves like a spin-0 or a scalar Bose gas significantly missing the rich phase properties. While in optical trapping, the interaction between the electric field of the laser beams and the dipole force of the neutral atoms favors in retaining the hyperfine spin states. Thus the system can be treated as spinor Bose gas which shows a plethora of interesting phase properties compared to the scalar Bose gas [2–9].

The dynamics of the ultracold atoms loaded in optical lattices were first theoretically analyzed by the well known Bose Hubbard Model (BHM) in a seminal paper by Jaksch *et. al.* [10] where the SF-MI phase transition is found to be completely governed by the competition between the hopping and two body interaction strengths.

Following this, different variants of BHM with nearest neighbor extended interactions [11–16], three and higher body interaction strengths [17–21], disorder [22–24] and multicomponent mixture of Bose gas [25, 26], superlattice potential [27, 28] etc have been studied. These studies nowadays contributes significantly for the exploration of the quantum gases. Needless to say disorder (or other inhomogeneities) play an important role in shaping the physics of such systems.

The general properties of spinor Bose condensates was first studied by Ho [3] and at the same time by Ohmi *et. al.* [4] where the system is characterized by a vector order parameter. The vector property of the condensate hence shows significant modification of the ground state structures and yields new topological excitations as compared to its scalar component. Later several studies on spinor Bose gas include the evolution of spin and singlet order parameters [29], spin orbit coupling [30–33], effects of disorder [34, 35] etc now under the lens from theoretical as well as experimental perspectives.

Recently due to the hyperfine spin states of spinor Bose gas, the creation of synthetic gauge fields and the observation of quantum Hall effect are of great importance where these zeeman sub levels act as a synthetic dimensions along the short axis against the optical lattice sites along the long axis [36, 37].

Besides that there are large number of literature review on spinor Bose gas under external magnetic fields which include the study of phase diagrams [5, 6], statistical physics of spin dynamics at finite temperature [38, 39], spatial and spin structures of ground state [40], phase separation [41], exact eigenstates [42] etc. Motivated by the studies carried out in Refs.[5, 6], where they consider the effect of external magnetic field only through the zeeman interaction term and show that the MI phase destabilizes with increasing field strength, here

\* saurabh@iitg.ernet.in

we consider the effect of the magnetic fields on both the hopping (via Peirls coupling) and the zeeman interaction terms for a chosen (Landau) gauge and see their competition on the MI-SF phase transition.

Apart from considering the effects of magnetic field, we feel it should be interesting to see the effects of three body interaction on spinor Bose gas, a topic which has not got enough attention. Unlike a scalar Bose gas, for a spinor Bose gas, the three body interaction strengths consists of two parts namely as, the three body spin independent and another one which is the spin dependent interaction terms as derived in Ref.[43].

In section II, we outline our theoretical model for a spinor Bose gas in presence of magnetic field and study it via the familiar mean field technique. In section III, we discuss the phase diagrams of the system in presence of the magnetic field and hence include a three body interaction potential to study an interplay between them. Finally we draw our conclusions in section IV.

## II. MODEL

The Hamiltonian for spin -1 ultracold atoms in presence of a magnetic field,  $B$  pointing in the  $z$  direction and enters through a vector potential  $\mathbf{A}$  chosen in the Landau gauge as,  $\mathbf{A} = Bx\hat{y}$ , is written as [3–6, 44],

$$H = - \sum_{\langle ij \rangle} \sum_{\sigma} (t_{i,j} a_{i\sigma}^{\dagger} a_{j\sigma} + h.c) - \mu \sum_i n_i + \frac{U_0}{2} \sum_i n_i (n_i - 1) + \frac{U_2}{2} \sum_i (\mathbf{S}_i^2 - 2n_i) + g\mu_B B \sum_i S_{iz} \quad (1)$$

Here  $t_{ij}$  is the hopping matrix elements from site  $i$  to nearest neighbour site  $j$  and is related to the magnetic vector potential  $\mathbf{A}$  via Peierls coupling as  $t_{ij} = -i \frac{2\pi}{\phi_0} \int_i^j \mathbf{A} \cdot d\mathbf{l}$  where  $\phi_0$  is the magnetic flux quantum. For a particular choice of the gauge field, the integral assumes the value as  $\phi = Bl_0^2/\phi_0$ ,  $l_0$  being the lattice spacing.  $a_{i\sigma}^{\dagger}$  ( $a_{i\sigma}$ ) is the boson creation (annihilation) operator at a site  $i$  and the particle number operator is  $n_i = \sum_{\sigma} n_{i\sigma}$ ,  $n_{i\sigma} = a_{i\sigma}^{\dagger} a_{i\sigma}$ .  $U_0$  is the spin independent and  $U_2$  is the spin dependent on-site interactions which are related to the scattering lengths  $a_{0,2}$  by  $U_0 = (4\pi\hbar^2/M)((a_0 + 2a_2)/3)$  and  $U_2 = (4\pi\hbar^2/M)((a_2 - a_0)/3)$  corresponding to  $S=0$  and  $S=2$  channels respectively [3, 4]. If the spin dependent interaction is  $U_2/U_0 > 0$ , then it is known as antiferromagnetic (AF) interaction and for  $U_2/U_0 \leq 0$ , it is known as ferromagnetic interaction. The total spin at a site  $i$  is given by,  $\mathbf{S}_i = a_{i\sigma}^{\dagger} \mathbf{F}_{\sigma\sigma'} a_{i\sigma'}$  where  $\mathbf{F}_{\sigma\sigma'}$  are the components of spin-1 matrices and  $\sigma = +1, 0, -1$ .  $\mu$  is the chemical potential,  $g$  is Lande g factor and  $\mu_B$  is the Bohr magneton and  $S_{iz} = a_{i+}^{\dagger} a_{i+} - a_{i-}^{\dagger} a_{i-} = n_{i+} - n_{i-}$  is the  $z$  component of  $\mathbf{S}_i$ . Here we consider a two dimensional square lattice where every lattice site  $i$  can be expressed by two indices as  $i = [l, m]$ ,  $l$  corresponds to lattice site

along  $x$  direction and  $m$  along  $y$  direction of the lattice.

To decouple the hopping term, we use the mean field approximation where the hopping term can be written as [45, 46],

$$a_{(l,m)\sigma}^{\dagger} a_{(l+1,m+1)\sigma} \simeq \langle a_{(l,m)\sigma}^{\dagger} \rangle a_{(l+1,m+1)\sigma} + a_{(l,m)\sigma}^{\dagger} \langle a_{(l+1,m+1)\sigma} \rangle \quad (2)$$

where  $\langle \rangle$  denotes the equilibrium value of an operator. Defining the superfluid order parameter at a site  $(l, m)$  as,  $\psi_{(l,m)\sigma} = \langle a_{(l,m)\sigma} \rangle$ , the total SF order parameter is given by  $\psi_{l,m} = \sqrt{\psi_{(l,m)\sigma}^2}$ . Substituting this in Eq.(1), the BHM can be written as a sum of single site Hamiltonians as,  $H = \sum_{l,m} H_{l,m}^{MF}$  where,

$$H_{l,m}^{MF} = - \sum_{\sigma} [t_{l+1,m} \psi_{l+1,m}^* a_{l,m} + t_{l-1,m} \psi_{l-1,m}^* a_{l,m} + t_{l,m+1} \psi_{l,m+1}^* a_{l,m} + t_{l,m-1} \psi_{l,m-1}^* a_{l,m} + h.c.] + \frac{U_0}{2} n_{l,m} (n_{l,m} - 1) + \frac{U_2}{2} (\mathbf{S}_{l,m}^2 - 2n_{l,m}) - \mu n_{l,m} + \eta [n_{(l,m)+} - n_{(l,m)-}] \quad (3)$$

where  $\eta = g\mu_B B$ . Using the Bloch periodic boundary condition and calculating the hopping matrix element between site  $(l, m)$  to a nearest neighbour  $(l \pm 1, m \pm 1)$ , we can write,

$$t_{l\pm 1, m\pm 1} \psi_{l\pm 1, m\pm 1} = \begin{cases} t \psi_{l\pm 1, m}; l, m = l \pm 1, m \\ t e^{\mp i 2\pi l \phi} \psi_{l, m}; l, m = n, m \pm 1 \end{cases} \quad (4)$$

Now to compute the ground state energy of the system, we first evaluate the matrix elements of the mean field Hamiltonian,  $H_{l,m}^{MF}$  in the occupation number basis,  $|n_{(l,m)\sigma}\rangle$  as,

$$\langle \hat{n}_{l,m+}, \hat{n}_{l,m0}, \hat{n}_{l,m-} | H_{l,m}^{MF} | \hat{n}_{l,m+}', \hat{n}_{l,m0}', \hat{n}_{l,m-}' \rangle = h_{l,m}^d + h_{l,m}^{od} \quad (5)$$

where the  $h_{l,m}^{od}$  correspond to the matrix elements coming from the off diagonal terms as,

$$h_{l,m}^{od} = -t \sqrt{n_{l,m}} [\psi_{l+1,m} + \psi_{l-1,m} + (e^{-i 2\pi l \phi} + e^{i 2\pi l \phi}) \psi_{l,m}] \quad (6)$$

and the diagonal part,  $h_{l,m}^d$  is calculated as

$$h_{l,m}^d = \frac{U_0}{2} n_{l,m} (n_{l,m} - 1) + \frac{U_2}{2} (\mathbf{S}_{l,m}^2 - 2n_{l,m}) - \mu n_{l,m} + \eta [n_{(l,m)+} - n_{(l,m)-}] \quad (7)$$

After diagonalizing Eq.(5) with  $n = 7$  for which  $\langle \hat{n}_{l,m+}, \hat{n}_{l,m0}, \hat{n}_{l,m-} | H_{l,m}^{MF} | \hat{n}_{l,m+}', \hat{n}_{l,m0}', \hat{n}_{l,m-}' \rangle$  is a  $120 \times 120$  matrix, we obtain the ground state energy,  $E_g(\psi_{l,m\sigma})$  and the eigenfunctions,  $\Psi_g(\psi_{l,m\sigma})$  starting with some guess value for  $\psi_{l,m\sigma}$ . Now from the updated wave function  $\Psi_g(\psi_{l,m\sigma})$ , we compute the equilibrium SF order parameter and local densities self consistently using,

$$\psi_{l,m\sigma} = \langle \Psi_g(\psi_{l,m\sigma}) | a_{l,m\sigma} | \Psi_g(\psi_{l,m\sigma}) \rangle \quad (8)$$

$$\rho_{l,m} = \langle \Psi_g(\psi_{l,m\sigma}) | n_{l,m\sigma} | \Psi_g(\psi_{l,m\sigma}) \rangle \quad (9)$$

It is relevant to mention that in absence of the magnetic field, the Hamiltonian is site independent and the SF order parameters are uniform over all the lattice sites, while in presence of magnetic field, they are site dependent and show a direct SF-MI phase transition caused by a competition among the hopping and interaction strengths. In the strong interaction limit, the system is in the MI phase which is basically a random phase with a vanishing SF order parameter and fixed number of bosons per lattice site. While at lower interaction strengths, the system switches over to the the conducting phase, that is the SF phase with finite SF order parameter and non integer occupation densities which can be perceived as an ordered phase.

### III. RESULTS

#### A. Magnetic field

Here we consider bosons in a magnetic field by choosing the magnetic flux to be expressible in the form of a rational fraction, that is,  $\phi = p/q$  where  $p, q$  are integers [44, 47]. In the chosen Landau gauge, from Eq.(5), the system is translationally invariant along the  $y$  direction and quasi periodic (as explained below) in the  $x$  direction. For a two dimensional square lattice with lattice site indices as  $(l, m)$ , the system maintains its periodicity along  $x$  direction with period  $l = q$ . This implies that we shall have to diagonalize the mean field Hamiltonian over a one dimensional chain of length  $q$ , that is, a  $1 \times q$  magnetic supercell with periodic boundary conditions in the  $x$  direction in order to obtain the ground state energy. Due to invariance along the  $y$  axis, the SF order parameter,  $\psi_{l,m}$  and occupation density,  $\rho_{l,m}$  are independent of  $m$  that is  $\psi_{l,m} = \psi_l$  and  $\rho_{l,m} = \rho_l$ . Further owing to the periodicity in the  $x$ -direction, we also have  $\psi_l = \psi_{l+q}$  and  $\rho_l = \rho_{l+q}$ . We shall obtain the phase diagram based on the site averaged SF order parameter,  $\bar{\psi} = \sum_q \psi(q)/q$  and local density,  $\bar{\rho} = \sum_q \rho(q)/q$  for different values of the magnetic flux,  $\phi$  [45].

The phase diagrams corresponding to the AF case with different value of  $\phi$  are shown in Fig.1(a). It shows that at low value of magnetic field strength, that is  $\phi = 0.05$ , the MI-SF phase boundary for the odd MI lobes shifts towards larger  $t/U_0$ , indicating a stabilization of the insulating phase while the same for the even MI lobes shows a decrease with  $t/U_0$ . In this case, for even MI lobes, the singlet pair formation continues to play a dominant role as pointed out in Ref.[48].

At large magnetic field strengths, say for example,  $\phi = 0.1$ , we found that the even MI lobes shrink noticeably while the other MI lobes are enhanced significantly, indicating further increase of the location for the MI-SF phase transition at this value of the field strength. This is quite interesting because the MI phase becomes more stable compared to the SF phase in comparison to the results obtained in Refs.[5, 6], where the effect of mag-

netic field enters in the Hamiltonian *only* through the zeeman interaction term. There it was observed that the insulating phase vanishes, pushing the system towards a SF region with increasing field strengths. In this work, at large magnetic fields, the zeeman interaction strength pushes the system towards the SF regime, while the magnetic flux included through the hopping term moves the system towards the MI regime. We explain this feature more clearly in the following discussion.

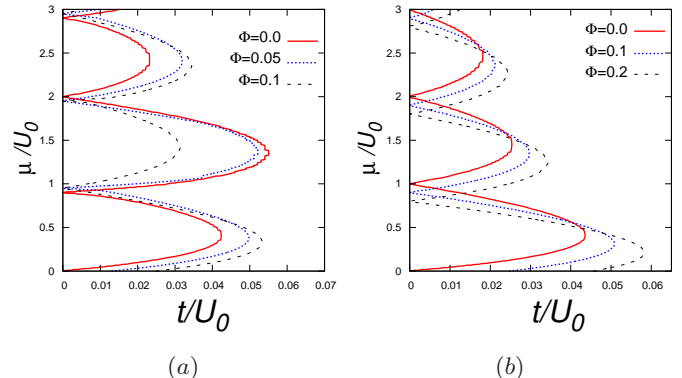


FIG. 1. (Color online) Phase diagrams for different values of  $\phi$  in antiferromagnetic case with  $U_2/U_0 = 0.05$  in (a) and for ferromagnetic case with  $U_2/U_0 = 0.0$  in (b). In AF case, at higher magnetic flux, the even MI lobes becomes unstable while odd MI lobes occupy more regime compared to the SF phase.

The Bose gas in presence of a magnetic field has an analogy with that of electrons on a thin film which suffer weak localization effects in a disordered environment [49]. Weak localization arises due to quantum interference of the paths traced by the conduction electrons scattered off the impurities. The presence of the magnetic field now introduces a relative phase difference arising among the time reversed paths, that is between the two interfering waves. This phase shift is random, and hence the magnetic field destroys the coherence of the interfering waves, thereby suppressing the interference pattern after a flight time proportional to  $1/B$ . Similar to the conduction electrons, for Bose systems, the magnetic flux tries to destroy the phase coherence of the SF order parameter near the transition point causing the system to move towards the MI regime. This explain a shift of the location for the MI-SF phase transition to larger value of  $t/U_0$  with increasing magnetic flux present in the hopping term.

Also the instability of the even MI lobes at higher magnetic flux values can be understood from the following discussion. At low magnetic fields, the formation of spin singlet (nematic) pair corresponding to the even (odd) MI lobes still continues and hence the ground state for even MI lobes is  $|0, 0, n\rangle$ , while for the odd MI lobes, it is  $|1, S_z, n\rangle$ . But at high field strengths, the ground state now changes from  $|0, 0, n\rangle$  to  $|2, S_z, n\rangle$  for the even MI lobes and  $|1, S_z, n\rangle$  to  $|3, S_z, n\rangle$  for the odd MI lobes, that is from  $S$  to  $S + 1$  since the formation of singlet or

the nematic pair no longer occur due to the change in ground state structure at higher value of the magnetic field strength in the zeeman term [5, 6].

The phase diagrams for the ferromagnetic case at  $U_2/U_0 = 0.0$  is shown in Fig.1(b). For the ferromagnetic interaction, the phase diagrams are similar to that of the spin-0 (scalar) system, except for only the chemical potential width now gets rescaled with the zeeman interaction strength,  $\eta$  as  $\mu + \eta \rightarrow \mu'$  [6, 45]. Unlike the antiferromagnetic case, in the ferromagnetic case, all the MI phases become more stable with increasing magnetic field strength due to the phase decoherence of the SF order parameter at the transition point as discussed above. Further each MI lobe now gets shifted along the vertical axis ( $\mu/U_0$ ) by an amount  $\eta/U_0$  due to rescaling of the chemical potential. The phase diagram at  $\phi = 0.1$  are in agreement with the results obtained in Ref.[45].

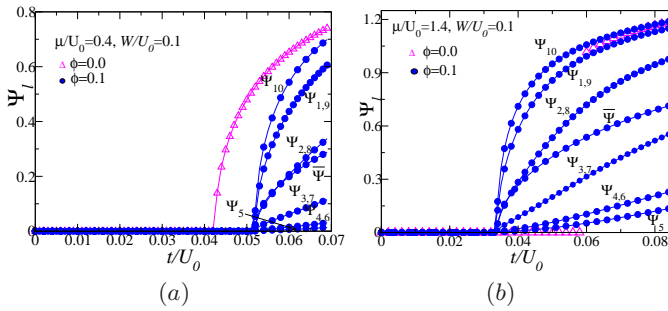


FIG. 2. (Color online) The 1D behaviours of  $\psi_l$  in AF case corresponding to odd MI lobe (a) and even (b) are shown with  $\phi$ . The MI-SF phase transition for odd MI lobe ( $\mu/U_0 = 0.4$ ) is second order for all values of  $\phi$  while for even MI lobes ( $\mu/U_0 = 1.4$ ), it is first order only when  $\phi \leq U_2/U_0$  but shows second order for higher magnetic flux *i.e.*  $\phi > U_2/U_0$ .

In Fig.2, we study the one dimensional behaviour of the SF order parameter corresponding to the even and the odd MI lobes in the antiferromagnetic case for different values of  $\phi$ . It is seen that the location of the MI-SF phase transition occurs at the same value of the hopping strength,  $t_c/U_0$  corresponding to different lattice sites  $l$  (of the magnetic supercell of dimension  $1 \times q$ ) and obeys the periodicity condition,  $\psi_l = \psi_{l+q}$ . Interestingly, for the odd MI lobes ( $\mu/U_0 = 0.4$ ), the MI-SF phase transition is second order in nature due to the continuous variation of the SF order parameter and increase in  $t_c/U_0$  value with increasing magnetic field strengths [Fig.2(a)]. While for even MI lobes ( $\mu/U_0 = 1.4$ ), for low magnetic field strengths, that is  $\phi \leq U_2/U_0$ , the MI-SF phase transition has a first order character due to jump in the order parameter. However for higher field strengths, that is  $\phi > U_2/U_0$ , the order parameter shows continuous variation from the MI to the SF phase and hence shows a second order transition for all  $\psi_l$ . Also the critical tunneling strength,  $t_c/U_0$  decreases with increasing magnetic flux values because of the absence of singlet pair formations [Fig.2(b)]. We have also studied  $\psi_l$  in the ferromagnetic case as a function of flux,  $\phi$  and the

results are in agreement with those obtained in Ref.[45].

## B. Three body interaction potential

We are also keen to explore the effect of three body interaction on spin-1 Bose gas which enters via the Hamiltonian (in addition to the Eq.(1)) as in the following [43],

$$H_3 = \frac{W}{6} \sum_i n_i(n_i - 1)(n_i - 2) + \frac{V}{6} \sum_i (\mathbf{S}_i^2 - 2n_i)(n_i - 2) \quad (10)$$

where  $W$  and  $V$  are the three body spin independent and dependent interaction strengths. It was found that the three body interaction strength is related with the two body interaction strength as,  $W \propto (V_0/E_r)^{3/4} a_s^2 k^2 U_0^2$  ( $a_s$ :  $s$  wave scattering length and  $k$ : wave vector) [18] and experimentally  $a_s^2 k^2$  is in the order of  $10^{-2}$  to  $10^{-8}$  [50]. Thus it is reasonable to consider  $W \ll U_0$  and the relationship,  $V/U_0 = 2(U_2/U_0)(W/U_0)$  only holds for  $W \ll U_0$  and  $V \ll U_2$  [43].

With these in hand, we study the effect of *only* the three body interaction before we go on to explore the consequences of magnetic field therein on the SF-MI phase transition.

Let us consider the atomic limit, that is  $t = 0$  on the spinor BHM in Eq.(10) without a magnetic field. At  $t = 0$ , the Hamiltonian consists only the unperturbed terms as,

$$H^0 = \frac{W}{6} n(n-1)(n-2) + \frac{V}{6} [S(S+1) - 2n](n-2) - \mu n + \frac{U_0}{2} n(n-1) + \frac{U_2}{2} [S(S+1) - 2n] \quad (11)$$

which has a common eigenstate  $|S, S_z, n\rangle$  where the corresponding operators, namely  $S, S_z, n$  commute with each other and we may remove the site index ( $l, m$ ) for the homogeneous case. In the atomic limit, the system is completely in the MI phase with an energy gap,  $E_g$  in the particle hole excitation spectra, which is the difference between the upper ( $\mu_+$ ) and lower ( $\mu_-$ ) values of the chemical potential corresponding to a MI lobe with occupancy  $n$  [51]. The  $\mu_{\pm}$  can be calculated from the following relation as  $E^0(S_1, n_1) < E^0(S, n) < E^0(S_2, n_2)$  where  $E^0$  is the eigenvalue of the  $H^0$  and  $S_{1,2}, n_{1,2}$  are the lower and higher spin and density values respectively corresponding to the  $S, n$  values. Following the calculation carried out in Ref.[34], this inequality corresponding to the antiferromagnetic case leads to following conditions, which are stated below.

- (i) For the odd MI lobes ( $n = 1, 3, \dots$ ):  $(n-1) + (n-1)(n-2)W/2U_0 + (1-n)V/3U_0 < \mu/U_0 < n - 2U_2/U_0 + n(n-1)W/2U_0 - (n-1)V/U_0$ . If we equate these two  $\mu$  values, we shall obtain a critical  $U_2/U_0$ , given by  $U_2^c/U_0 = 1/2 + (n-1)[W/2U_0 - V/3U_0]$  below which the odd MI lobes exist and above which the odd MI lobes vanish.
- (ii) For even MI lobes ( $n = 2, 4, \dots$ ): If  $U_2/U_0 < U_2^c/U_0$

(as above), then  $(n-1) - 2U_2/U_0 + (n-1)(n-2)W/2U_0 + (2-n)V/U_0 < \mu/U_0 < n + n(n-1)W/2U_0 - nV/3U_0$ . For  $U_2/U_0 > U_2^c/U_0$ ,  $n - 3/2 - U_2/U_0 + (n-2)^2W/2U_0 + 2(2-n)V/3U_0 < \mu/U_0 < n + 1/2 - U_2/U_0 + n^2W/2U_0 - 2nV/3U_0$ .

Similarly for the ferromagnetic case, since there is no distinction between the odd and even MI lobes, for all MI lobes,  $(n-1)[1 + U_2/U_0 + (n-2)W/2U_0 + (n-2)V/2U_0] < \mu/U_0 < n[1 + 2U_2/U_0 + (n-1)W/2U_0 + (n-1)V/2U_0]$ .

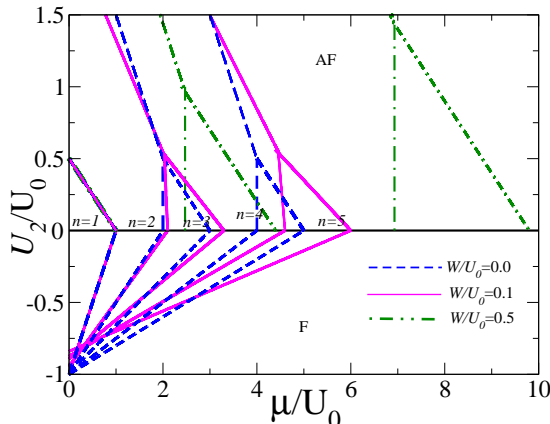


FIG. 3. (Color online) The MI lobe structures at the atomic limit that is  $t = 0$  with  $W/U_0$  both in the antiferromagnetic and the ferromagnetic cases.

If we plot all these equations for different values of  $W/U_0, V/U_0$ , we shall obtain the MI lobe structures as shown in Fig.3. In the AF case, for  $W/U_0 = 0.1$  which yields  $V/U_0 = 0.2U_2/U_0$  and we found that the even MI lobes become more stable compared to the odd MI lobes and the width of the chemical potential,  $\mu$  for all the MI lobes, except the first one, increases with the three body interaction strength,  $W$ , suggesting the dominance of the insulating phase compared to the SF phase. Interestingly, the critical  $U_2^c/U_0$  for the disappearance for all odd MI lobes in absence of  $W/U_0$  was 0.5 [34] now changes to 0.53 and 0.553 at  $W/U_0 = 0.1$  corresponding to the third and fifth odd MI lobes respectively.

We have also considered a higher value of the three body interaction strength that is  $W/U_0 = 0.5$ , for which we have chosen  $V/U_0 = 0.05 \sim U_2/U_0$  and found that the chemical potential boundary gets enhanced, thereby making inroads for the MI phase to be more stable. This is particularly true for the even MI lobes where the critical value,  $U_2^c/U_0$  increases accordingly with  $W, V$ .

In the ferromagnetic case, the MI phase has similar properties like a spin-0 (scalar) Bose gas and the increase of the right boundary of chemical potential in Fig.3 results in the increase in second and higher MI lobes width with inclusion of three body interaction potential.

Now we turn on the hopping strengths and present the phase diagrams obtained from mean field approximation (MFA) (see Eq.(5)) in order to study the SF-MI transition with three body interaction strengths. The phase

diagrams corresponding to the AF case for  $U_2/U_0 = 0.05$  with different values of  $W/U_0$  are shown in Fig.4. At  $W/U_0 = 0.1$ , we found that although there is no change for the first MI lobe, but the second and higher MI lobes get enhanced with  $W/U_0$  as seen from Fig.3. With increasing the three body interaction strength,  $W/U_0$ , the MI phase now encroaches more towards the SF regime, pushing the system to an insulating phase rather than a conducting phase. The phase diagram without  $W/U_0$  is included for comparison which was studied earlier in Refs.[46, 48]. Besides, the location for the MI-SF phase transition is now occurring at higher values of hopping strength,  $t_c/U_0$  due to the presence of three body interaction strength.

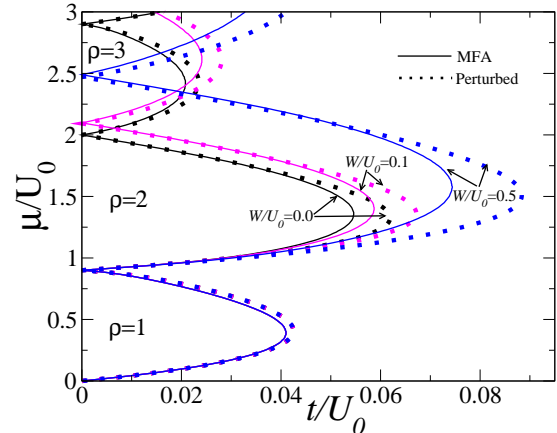


FIG. 4. (Color online) Phase diagrams in the AF case with  $U_2/U_0 = 0.05$  for  $W/U_0 = 0.1$  and 0.5. The solid lines are for the mean field results and the dotted lines are obtained via perturbed method.

Thus adding higher interaction strengths (such as a four body term etc) in the Hamiltonian, the effect is that the system acquires higher interaction energy which requires large hopping strengths to overcome this potential blockade. We have also checked that the first and third odd MI lobes vanish when the spin dependent interaction value satisfies,  $U_2/U_0 = 0.54 \geq U_2^c/U_0$  at  $W/U_0 = 0.1$  and  $U_2^c/U_0 = 0.967$  for  $W/U_0 = 0.5$ . These numbers are in agreement with the analytic calculations presented earlier for the atomic limit corresponding to the disappearance of the respective MI lobes.

The variation of SF order parameter,  $\psi$  and local density,  $\rho$  corresponding to the AF case including  $W/U_0$  are shown in Fig.6(a). The chemical potential,  $\mu/U_0$  for the SF-MI phase transition corresponding to the first odd MI lobe [MI(1)] remains unaltered, while for the other MI lobes, it increases with the three body interaction strength,  $W/U_0$ . Also for the even MI phase, the MI-SF phase transition still has a first order character and for the odd MI phase, it is a second order phase transition as ascertained earlier in Ref.[46] without  $W/U_0$ .

The mean field phase diagrams corresponding to the ferromagnetic case with  $U_2/U_0 = 0.0$  is shown in Fig.5.

It has similar phase properties like a scalar Bose gas. As seen from Fig.3, since the chemical potential width,  $\mu/U_0$  now increases with the three body interaction strength for the second ( $n = 2$ ) and further higher order MI lobes, thus all the MI lobes, except the first one, occupy more and more space in the phase diagram compared to the SF phase. Also the critical hopping strength,  $t_c/U_0$  for the SF-MI transition increases with  $W/U_0$ . The behaviour of  $\psi$  and  $\rho$  also shown in Fig.6(b) where the value of the chemical potential increases with  $W/U_0$  and the SF-MI phase transition still remains second order in presence of the three body interaction [46].

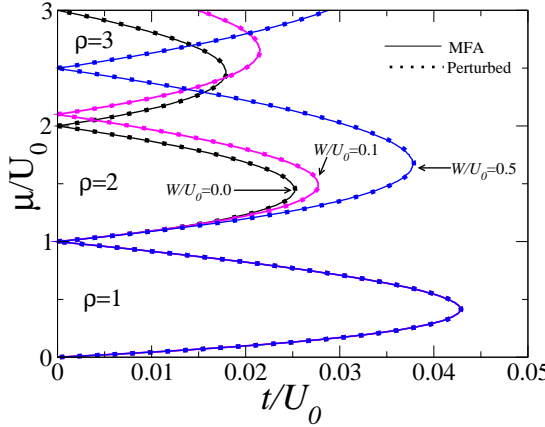


FIG. 5. (Color online) Phase diagrams corresponding to the ferromagnetic case with  $U_2/U_0 = 0.0$  for  $W/U_0 = 0.1$  and  $0.5$ . The solid lines are for the mean field results and the dotted lines are obtained via perturbated method.

Now we shall do a perturbation calculation to provide a strong support for all of these mean field phase diagrams computed numerically. Further we shall ascertain the location of the MI-SF phase transition including the three body interaction potential,  $W/U_0$ . After applying the mean field approximation, the perturbed Hamiltonian is given by  $H' = -t \sum_{\sigma} [a_{\sigma}^{\dagger} \psi_{\sigma} + h.c] + t \sum_{\sigma} \psi_{\sigma}^2$ . Using the same eigenstate as that of  $H^0$ , the change in the ground state energy, after incorporating the first and second order corrections, can be expressed in a series expansion for  $\psi$  as,

$$E_g(\psi) = E^0 + E^1 + E^2 \\ = E^0 + A_2(U_0, U_2, \mu, n, W, V) \sum_{\sigma} \psi_{\sigma}^2 + O(\psi^4) \quad (12)$$

where the coefficient,  $A_2(U_0, U_2, \mu, n, W, V)$  includes the first and second order corrections for a particular spin component  $\sigma$ . Minimizing the ground state energy with respect to  $\psi$  leads to  $A_2(U_0, U_2, \mu, n, W, V) = 0$  and this equation yields the boundary between the SF to MI phases.

In the AF case, for the even MI lobes, using a non degenerate perturbation theory as done in Ref.[48], the SF-MI phase boundary can be obtained via

$A_2(U_0, U_2, \mu, n, W, V) = 0$ . The above equation gives

$$t^{-1} = \frac{n/3}{\mu + 2U_2 - (n-1)U_0 - (n-2)[(n-1)W/2 + V]} \\ + \frac{(n+3)/3}{nU_0 - \mu + n(n-1)W/2 - nV/3} \quad (13)$$

Similarly for the odd MI lobes, one gets,

$$t^{-1} = \frac{(n+2)/3}{\mu - (n-1)[U_0 + (n-2)W/2 - V/3]} + \\ \frac{4(n-1)/15}{\mu + 3U_2 - (n-1)[U_0 + (n-2)W/2] - (4n-10)V/3} \\ + \frac{(n+1)/3}{-\mu + nU_0 - 2U_2 + (n-1)[nW/2 - V]} \\ + \frac{4(n+4)/15}{-\mu + U_2 + nU_0 + (n^2 - n)[W/2 - 2V/3]} \quad (14)$$

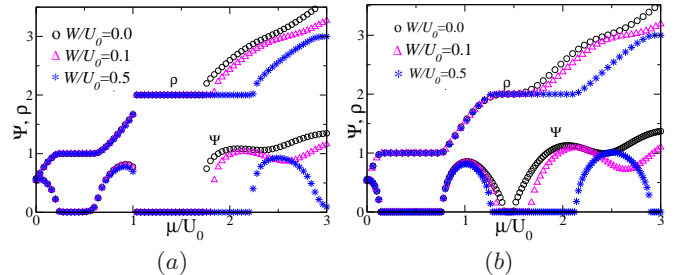


FIG. 6. (Color online) The variation of  $\psi$  and  $\rho$  with  $W/U_0$  for the antiferromagnetic case is shown in (a) and the ferromagnetic case is shown in (b).

If we plot these two equations with different values of  $W, V$  at  $U_2/U_0 = 0.05$  corresponding to the MI lobe with occupancy,  $n$  we obtain the phase diagrams as shown in Fig.4. At  $W/U_0 = 0.1$ , we found that the phase diagrams obtained using this perturbation approach are in good agreement with the mean field phase diagrams deep inside the MI lobes. However near the tip of the MI lobes, the mean field and phase diagrams obtained via this technique differ from each other. This is because the mean field approach is not a very appropriate tool to handle fluctuations and are in fact quite inadequate at the transition point for the MI-SF phase boundary [48] and the deviation increases with increasing  $W/U_0$ .

If we solve the above equations, which are quadratic in  $\mu$  shows that the critical hopping strength,  $t_c/U_0$  (by equating  $\mu_+$  and  $\mu_-$ ) which denotes the location for the MI-SF phase transition is now a function of  $W$  and  $V$  and increases with the three body interaction strength,  $W$ .

Similarly in the ferromagnetic case, we have performed similar perturbation calculation and at  $U_2/U_0 = 0$  the obtained phase diagrams are in complete agreement with the mean field ones corresponding to different values of  $W/U_0$  and they are shown in Fig.5.

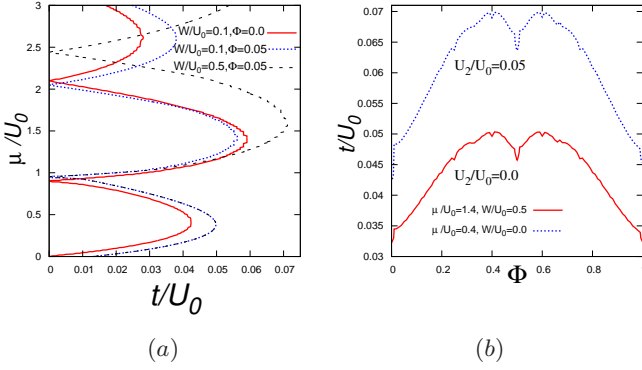


FIG. 7. (Color online) Phase diagrams in the antiferromagnetic case with  $U_2/U_0 = 0.05$  and  $W/U_0$  for different values of  $\phi$  is shown in (a). Also the phase diagram for complete range of  $\phi$  in the antiferromagnetic and ferromagnetic cases is shown in (b) shows a mirror symmetry about  $\phi = 0.5$ .

Finally we incorporate the effect of the magnetic field and compute the phase diagrams in presence of a three body interaction potential for different values of  $\phi$  and are shown in Fig.7(a). It shows similar effect (as without  $W$ ) with increasing magnetic flux strength as discussed earlier. Here the MI phase now experiences robustness compared to the SF phase due to the presence of  $W/U_0$ . We have also studied the SF-MI phase transition in the ferromagnetic case corresponding to  $W/U_0$  with different values of  $\phi$ . Another interesting property that we have obtained is the symmetry of phase diagram as a function of  $\phi$ . The energy spectrum is identical for  $\phi$  and  $N + \phi$  where  $N$  is an integer and is symmetric under  $\phi = -\phi$  as studied in Ref.[47]. This is seen in Fig.7(b), where we consider the flux over a period of  $[0,1]$  which shows a reflection symmetry around  $\phi = 0.5$  both in the antiferromagnetic and the ferromagnetic cases and in agreement with results in Ref.[45] for the ferromagnetic case.

#### IV. CONCLUSION

In this work, we have elaborately studied the effect of an external magnetic field and a repulsive three body interaction potential on spin-1 ultracold Bose gas. At first, we have obtained the phase diagrams in presence of magnetic field corresponding to both types of spin dependent interactions. In the AF case, at low magnetic field strengths, the even MI lobes continue to play a dominant role compared to the odd MI lobes due to formation of spin singlet pairs. While at higher magnetic field strengths, the zeeman interaction term suppresses the singlet pairs formation and thereby destabilizes the even MI lobes. However the effect of magnetic field in the hopping term, included via  $e^{if(\phi)}$  ( $\phi$  being the flux), pushes the system towards the MI regime. As a result, the odd MI lobes encroach into the SF regime. In the ferromagnetic case, the phase diagrams are similar to that of the scalar Bose gas and the system is more likely to

be in the MI regime compared to the SF phase with increasing flux strengths. Also the nature of MI-SF phase transition for the even MI lobes is first order as long as flux is less than the spin dependent interaction (scaled by  $U_0$ ) but changes over to a second order transition for higher flux strengths in the AF case.

Next we consider the effect of a three body interaction strength without the magnetic field and found that the chemical potential width is enhanced and hence the MI phase occupies more region compared to the SF phase. In the AF case, the even MI lobes become more stable compared to the odd MI lobes and the odd MI lobes vanish when the spin dependent interaction term is greater than a certain critical value. The location of the critical tunneling strength for the MI-SF phase transition also increases (towards larger  $t/U_0$ ) with the strength of the three body interaction term.

Experimentally the three and higher body interaction terms were successfully observed using atom interferometry as studied in Ref.[52] and photon assisted tunneling in Ref.[53]. Also it has been proposed to observe three body interaction effects using an optical lattice and superlattice potential in Ref.[28]. Recently Paul *et. al.* successfully engineered a Bose Hubbard Hamiltonian with an attractive three body interaction potential which is dominant than the two body interaction potential [54].

A perturbation calculation has also been done to provide a support for the mean field phase diagrams. In the AF case, the phase diagrams obtained via perturbation calculation are in good agreement with the mean field approach deep inside the MI regime, but they differ near the tip of the MI lobes and the discrepancy becomes noticeable with increasing value of three body interaction strength. While in the ferromagnetic case, the mean field phase diagrams are in complete agreement with those obtained using the perturbed calculation.

We have also studied the SF-MI phase transition with a three body interaction term corresponding to different values of the magnetic flux and they show similar properties as that corresponding to the case without a three body interaction term. Besides, the system shows a reflection symmetry about  $\phi = 0.5$  both for the antiferromagnetic and the ferromagnetic cases over a period of  $\phi \in [0, 1]$ .

However all the experimental results cited above are relevant to the scalar Bose gas. We have a strong conviction that our theoretical results on the spinor Bose gas will be useful to ascertain many of the interesting phenomena that are otherwise absent in the scalar Bose gas.

#### ACKNOWLEDGMENTS

SNN likes to thank Prof. M. Oktel and Dr. O. Umucalilar for their help. We thank Prof. R. V. Pai for useful discussions. SB thanks CSIR, India for financial support under the grants F no: 03(1213)/12/EMR-II.

---

[1] M. Greiner, O. Mandel, T. Esslinger, T. W. Hansch, and I. Bloch, *Nature* **415**, 39 (2002).

[2] D. M. Stamper-Kurn, M. R. Andrews, A. P. Chikkatur, S. Inouye, H.-J. Miesner, J. Stenger, and W. Ketterle, *Phys. Rev. Lett.* **80**, 2027 (1998).

[3] T.-L. Ho, *Phys. Rev. Lett.* **81**, 742 (1998).

[4] T. Ohmi and K. Machida, *J. Phys. Soc. Jpn.* **67**, 1822 (1998).

[5] A. A. Svidzinsky and S. T. Chui, *Phys. Rev. A* **68**, 043612 (2003).

[6] N. Uesugi and M. Wadati, *J. Phys. Soc. Jpn.* **72**, 1041 (2003).

[7] C. K. Law, H. Pu, and N. P. Bigelow, *Phys. Rev. Lett.* **81**, 5257 (1998).

[8] E. Demler and F. Zhou, *Phys. Rev. Lett.* **88**, 163001 (2002).

[9] T. Kimura, S. Tsuchiya, and S. Kurihara, *Phys. Rev. Lett.* **94**, 110403 (2005).

[10] D. Jaksch, C. Bruder, J. I. Cirac, C. W. Gardiner, and P. Zoller, *Phys. Rev. Lett.* **81**, 3108 (1998).

[11] P. Sengupta, L. P. Pryadko, F. Alet, M. Troyer, and G. Schmid, *Phys. Rev. Lett.* **94**, 207202 (2005).

[12] T. Mishra, R. V. Pai, S. Ramanan, M. S. Luthra, and B. P. Das, *Phys. Rev. A* **80**, 043614 (2009).

[13] M. Iskin, *Phys. Rev. A* **83**, 051606 (2011).

[14] T. Ohgroe, T. Suzuki, and N. Kawashima, *Phys. Rev. B* **86**, 054520 (2012).

[15] A. Barman and S. Basu, *J. Phys. B: At. Mol. Opt. Phys.* **46**, 125303 (2013).

[16] A. Barman and S. Basu, *J. Phys. B: At. Mol. Opt. Phys.* **46**, 125303 (2013).

[17] K. P. Schmidt, J. Dorier, and A. M. Läuchli, *Phys. Rev. Lett.* **101**, 150405 (2008).

[18] B.-l. Chen, X.-b. Huang, S.-p. Kou, and Y. Zhang, *Phys. Rev. A* **78**, 043603 (2008).

[19] S. Ejima, F. Lange, H. Fehske, F. Gebhard, and K. z. Münster, *Phys. Rev. A* **88**, 063625 (2013).

[20] K. W. Mahmud, E. Tiesinga, and P. R. Johnson, *Phys. Rev. A* **90**, 041602 (2014).

[21] T. Sowiński, R. W. Chhaunjany, O. Dutta, L. Tagliacozzo, and M. Lewenstein, *Phys. Rev. A* **92**, 043615 (2015).

[22] U. Bissbort, R. Thomale, and W. Hofstetter, *Phys. Rev. A* **81**, 063643 (2010).

[23] A. E. Niederle and H. Rieger, *Phys. Rev. A* **91**, 043632 (2015).

[24] P. Buonsante, L. Pezzè, and A. Smerzi, *Phys. Rev. A* **91**, 031601 (2015).

[25] G.-H. Chen and Y.-S. Wu, *Phys. Rev. A* **67**, 013606 (2003).

[26] F. Lingua, M. Guglielmino, V. Penna, and B. Capogrosso Sansone, *Phys. Rev. A* **92**, 053610 (2015).

[27] B.-L. Chen, S.-P. Kou, Y. Zhang, and S. Chen, *Phys. Rev. A* **81**, 053608 (2010).

[28] M. Singh, A. Dhar, T. Mishra, R. V. Pai, and B. P. Das, *Phys. Rev. A* **85**, 051604 (2012).

[29] S. S. Natu, J. H. Pixley, and S. Das Sarma, *Phys. Rev. A* **91**, 043620 (2015).

[30] L. Wen, Q. Sun, H. Q. Wang, A. C. Ji, and W. M. Liu, *Phys. Rev. A* **86**, 043602 (2012).

[31] L. Chen, H. Pu, and Y. Zhang, *Phys. Rev. A* **93**, 013629 (2016).

[32] K. Sun, C. Qu, Y. Xu, Y. Zhang, and C. Zhang, *Phys. Rev. A* **93**, 023615 (2016).

[33] J. H. Pixley, S. S. Natu, I. B. Spielman, and S. Das Sarma, *Phys. Rev. B* **93**, 081101 (2016).

[34] M. Łącki, S. Paganelli, V. Ahufinger, A. Sanpera, and J. Zakrzewski, *Phys. Rev. A* **83**, 013605 (2011).

[35] S. N. Nabi and S. Basu, *J. Phys. B: At. Mol. Opt. Phys.* **49**, 125301 (2016).

[36] A. Celi, P. Massignan, J. Ruseckas, N. Goldman, I. B. Spielman, G. Juzeliūnas, and M. Lewenstein, *Phys. Rev. Lett.* **112**, 043001 (2014).

[37] B. K. Stuhl, H.-I. Lu, L. M. Aycock, D. Genkina, and I. B. Spielman, *Science* **349**, 1514 (2015).

[38] K. Kis-Szabó, P. Szépfalusy, and G. Szirmai, *Phys. Rev. A* **72**, 023617 (2005).

[39] G. Lang and E. Witkowska, *Phys. Rev. A* **90**, 043609 (2014).

[40] M. Matuszewski, *Phys. Rev. A* **82**, 053630 (2010).

[41] M. Matuszewski, T. J. Alexander, and Y. S. Kivshar, *Phys. Rev. A* **80**, 023602 (2009).

[42] M. Koashi and M. Ueda, *Phys. Rev. Lett.* **84**, 1066 (2000).

[43] K. W. Mahmud and E. Tiesinga, *Phys. Rev. A* **88**, 023602 (2013).

[44] M. Niemeyer, J. K. Freericks, and H. Monien, *Phys. Rev. B* **60**, 2357 (1999).

[45] M. O. Oktel, M. Niža, and B. Tanatar, *Phys. Rev. B* **75**, 045133 (2007).

[46] R. V. Pai, K. Sheshadri, and R. Pandit, *Phys. Rev. B* **77**, 014503 (2008).

[47] D. R. Hofstadter, *Phys. Rev. B* **14**, 2239 (1976).

[48] S. Tsuchiya, S. Kurihara, and T. Kimura, *Phys. Rev. A* **70**, 043628 (2004).

[49] G. Bergmann, *Phys. Rep.* **107**, 1 (1984).

[50] C. J. Pethick and H. Smith, *Bose-Einstein Condensation in Dilute Gases*, Cambridge University Press, Cambridge, England, 2002.

[51] M. P. A. Fisher, P. B. Weichman, G. Grinstein, and D. S. Fisher, *Phys. Rev. B* **40**, 546 (1989).

[52] S. Will, T. Best, U. Schneider, L. Hackermüller, D.-S. Luhmann, and I. Bloch, *Nature* **465**, 197 (2010).

[53] R. Ma, M. E. Tai, P. M. Preiss, W. S. Bakr, J. Simon, and M. Greiner, *Phys. Rev. Lett.* **107**, 095301 (2011).

[54] S. Paul, P. R. Johnson, and E. Tiesinga, *Phys. Rev. A* **93**, 043616 (2016).